https://doi.org/10.5194/bg-2019-444
Preprint. Discussion started: 16 December 2019
© Author(s) 2019. CC BY 4.0 License.

Biogeosciences Discussions
Open Access
EGU

Calcite and vaterite biosynthesis by nitrate dissimilating bacteria in carbonatogenesis process under aerobic and anaerobic conditions

Marwa Eltarahony[1], Sahar Zaki[1]*, Ayman Kamal[1], Desouky Abd-El-Haleem[1]

[1]Environmental Biotechnology Department, Genetic Engineering and Biotechnology Research Institute (GEBRI), City of Scientific Research and Technological Applications (SRTA-City), 21934, New Borg El-Arab City, Alexandria, Egypt

Correspondence to: Sahar A. Zaki (saharzaki@yahoo.com)

https://doi.org/10.5194/bg-2019-444
Preprint. Discussion started: 16 December 2019
© Author(s) 2019. CC BY 4.0 License.

Biogeosciences Discussions Open Access EGU

Abstract

This study deals with 16S rDNA identified bacteria, *Lysinibacillus sphaericus* (71A), *Raoultella planticola* (VIP), and *Streptomyces pluricolorescens* (EM4) capable of precipitating $CaCO_3$ through a nitrate reduction aerobically and anaerobically. The produced $CaCO_3$ crystals were analyzed using XRD, EDX, and SEM. The results showed that the carbonatogenic bacteria served as nucleation sites for $CaCO_3$ precipitation with distinct variation in polymorph and morphology; reflecting strain-specific property. Notably, the amount of precipitated $CaCO_3$ recorded 3.27 (aerobic), 1.55 (anaerobic), 4.15 (aerobic), 3.75 (aerobic) and 1.87 (anaerobic) g/100 mL of strains 71A, EM4 and VIP, respectively, for 240h of incubation. The study of changes in media chemistry during carbonatogenesis process revealed positive correlation between bacterial growth, nitrate reductase activity, pH, EC, amount of deposited $CaCO_3$ and NO_3^- consumption. Therefore, the applications of these bacterial strains, which employed for the first time in carbonatogenesis process, are promising in the environmental, biomedical and civil engineering fields.

Key words: *Streptomysetes*, $CaCO_3$ biodeposition, carbonatogensis process, nitrate reduction, biocementation.

https://doi.org/10.5194/bg-2019-444
Preprint. Discussion started: 16 December 2019
© Author(s) 2019. CC BY 4.0 License.

1. Introduction

Biomineralization is a process of inorganic mineral deposition by living organisms, which occurs naturally at a slow rate over geological times. Microorganisms mediate the biomineralization process through a sequence of biochemical activities and physiological pathways, which alter the chemical environment and ultimately lead to mineral precipitation (**Chaparro-Acuña et al., 2018)**, by two main different mechanisms; biologically controlled mineralization (BCM) and biologically induced mineralization (BIM) **(Ghosh et al., 2019, Wei et al., 2015; Anbu, et al., 2016**).

Interestingly, Microbial induced calcium carbonate precipitation (MICCP) which also called carbonatogenesis attracted a considerable attention in various biotechnological applications. Carbonatogenesis is an eco-friendly and cost-effective technology that can be applied to remediate various environmental pollution originated from anthropogenic activities (**Rodriguez-Navarro et al., 2012)**. As referred by **Chaparro-Acuña et al., (2018).** It enhances water quality in water softening process, which subsequently participates in solving water crisis problem. On industrial level, calcium carbonates have been widely used as viscosity modifier in plastics, rubber, inks, paint, paper and pigment products (**Anbu et al., 2016**). For medical and therapeutic sectors, it has been utilized in drug delivery and tissue engineering **(Poelvoorde, 2017)**. Recently, microbial $CaCO_3$ paved the way for new subdiscipline in biotechnology, which is construction microbial biotechnology, including biocrusting, and biocementation **(O'Donnell et al., 2019**).

Naturally, calcium carbonate occurs on earth's surface, and contributes mainly in geochemical reservoir for carbon **(Hu et al., 2012)**. It exists in various polymorphs with distinct characteristics, including vaterite (the most thermodynamically unstable and the highest solubility spherical like), aragonite (the densest and thermodynamically unstable needle like), calcite (the most stable rhombic), two hydrated crystalline phases, monohydrocalcite, ikaite and amorphous phases (**Sevcık et al., 2018**). The metastable phases can be easily recrystallized to stable calcite phase **(Han et al., 2017)**. As reported in extensive studies (**Ersan et al., 2015**, **Ghosh et al., 2019**), different microorganisms precipitated different types of $CaCO_3$.

https://doi.org/10.5194/bg-2019-444
Preprint. Discussion started: 16 December 2019
© Author(s) 2019. CC BY 4.0 License.

The calcifying microorganisms stimulate $CaCO_3$ precipitation via two fundamental mechanisms either autotrophic or heterotrophic (**Singh, 2019)**; which seems to be more abundant. Photosynthetic microorganisms fix CO_2 and induce carbonate precipitation autotrophically (**Richardson et al., 2014**). Conversely, three main categories of microorganisms induce biocalcification process heterotrophically. The first category catalyzes the reduction of sulphate by sulphate reducing bacteria (SRB) **(Lin et al., 2018).** The second category comprises microorganisms, which participate in nitrogen cycle by one of the following means: A)- oxidative deamination of amino acids, B)- nitrate reduction C)- urea hydrolysis (**Richardson et al., 2014)**. The third category promotes the reversible conversion of CO_2 to bicarbonate through carbonic anhydrase enzyme (**Zhu and Dittrich 2016**).

Remarkably, the majority of studies concerned with calcification technology focused on ureolysis processes and few researches were performed on nitrate dissimilation metabolism (**Zhu and Dittrich 2016).** Nonetheless, ureolysis processes exhibited several limitations, namely; the byproduct of urea hydrolysis (ammonia or ammonium), which is potentially hazardous, requires removal later on by another stage **(O'Donnell et al., 2019)**. Moreover, the using of aerobic urolytic bacteria *in situ* will result in calcite disintegration due to oxygen shortage and changing in pH surrounding to bacteria, which eventually lead to insufficient applications **(Thirumalai, 2015)**. Interestingly, carbonatogenesis via dissimilatory nitrate reduction deemed as remarkable alternative mechanism that can overcome the drawbacks of ureolysis. Where, nitrate dissimilatory microorganisms are more prevalent in the subsurface and display flexibility in their growth strategy; they are able to utilize low NO_3^- concentrations under anoxic conditions and without formation of harmful or toxic byproducts. Besides, denitrification is thermodynamically more favorable than ureolysis. As refereed by **Ersan et al., 2015,** the change in standard Gibbs energy for denitrification is -785 kJ/mol acetate, while it was estimated to be -27 kJ/mol acetate for ureolysis. Furthermore, the carbonate yield generated by denitrification process is higher than ureolysis**.**

Accordingly, the present study aimed to determine the carbonate precipitation efficiency of heterotrophic nitrate dissimilating bacteria under both aerobic and anaerobic conditions. The selected

https://doi.org/10.5194/bg-2019-444
Preprint. Discussion started: 16 December 2019
© Author(s) 2019. CC BY 4.0 License.

nitrate reducing-bacteria under study were isolated from Egyptian non-calcareous habitats and identified by 16S rDNA gene sequencing. The substantial part of this study focused on characterization of $CaCO_3$ precipitated by each strain under oxic and anoxic conditions, which will check the suitability of each CaCO3 crystals considering their prospective application according to mineralogy and morphology. Subsequently, different criteria such as bacterial count, nitrate reductase (NR) activity, pH, deposited $CaCO_3$ amount, NO_3^- concentration, NO_2^- concentration and electrical conductivity (EC) were analyzed. As far as the authors know, it is the first report of carbonatogenesis process through nitrate reduction under aerobic and anaerobic conditions.

2. Materials and Methods

2.1. Sampling, screening and selection of nitrate-reducing bacteria

Sediment samples were collected from non-calcareous Egyptian sites; Naba Alhamra at Wadi Elnatron (Al-Beheira governorate), Karon Lake (Al-Fayoum governorate) and Mariot Lake (Alexandria governorate). Directly after sampling, isolation and screening of bacteria for nitrate reduction were performed. Initially, 1 g of fine powdered homogenized samples were serially diluted in 0.85 % saline, and then plated on denitrifying media containing bromothymol blue and incubated aerobically (**Lv et al., 2017)**. The bacterial isolates that reduced nitrate aerobically were picked up and re-examined for nitrate reduction under anaerobic conditions as described by **Zaki et al. (2019)**. Out of 17 nitrate reducing-bacteria, three isolates, designated as 71A, VIP and EM4 were selected based on their nitrate reduction capabilities. Generally, nitrate reductase (NR) assay performed using spectrophotometric measurement of nitrite concentration at 540 nm. This was based on diazo-coupling method with Griess reagents (0.2 % Naphthyl ethylenediamine and 2% Sulfanilamide in 5% phosphoric acid). Nitrite generated from nitrate in presence of 40 mM of an artificial electron donor dithionite benzyle viologen. One unit of NR activity corresponds to the amount of enzyme that catalyzes the formation of 1µmol of nitrite per minute or 1µmol of nitrate reduced per minute under standard assay conditions **(Zaki et al., 2019)**.

2.2. Molecular identification of selected isolates

https://doi.org/10.5194/bg-2019-444
Preprint. Discussion started: 16 December 2019
© Author(s) 2019. CC BY 4.0 License.

The selected isolates were identified using16S rDNA sequencing. The bacterial genomic DNAs of the selected isolates were extracted from overnight pure cultures and 16S rDNA genes were PCR amplified, purified and sequenced as described elsewhere **(Vashisht et al., 2018).** The phylogenetic affiliation was inquired by applying BLAST analysis to determine the similarities with their available GenBank database sequences. Their generated sequences were submitted to the GenBank to obtain corresponding accession numbers. For multiple alignment and phylogenetic tree construction, the software package MEGA- 6 was employed.

2.3. $CaCO_3$ precipitation and crystals collection

The capability of selected isolates for $CaCO_3$ precipitation through nitrate reduction process was assessed in liquid broth method at flask level. About 250 µL of bacterial cultures (1.8 x 10^6 CFU/mL) were inoculated in 200 ml $CaCO_3$ precipitation media (CCP) which composed of M9 media supplemented with (g/L): sodium acetate (10) and Ca $(NO_3)_2 \cdot 4H_2O$ (15) at pH 7.0 ± 2.2 **(Ersan et al., 2015)**. The flasks were incubated aerobically in an orbital shaker at 150 rpm and anaerobically as stated by **Zaki et al., (2019**). The inoculated flasks were incubated at 30°C for 10 days. An abiotic negative control consisted of un-inoculated media was run in parallel. At the end of the experiment, the whole cultures were centrifuged at 10.000g for 20 min and washed successive times by distilled water and ethanol to eliminate any nutritive solution. The air-dried minerals were weighted to estimate the amount of precipitated $CaCO_3$ and subsequently subjected to mineralogical studies **(Vashisht et al., 2018).**

2.4. Mineralogical and morphological analysis

The mineralogical analysis of the dried precipitated $CaCO_3$ was established with X-ray diffraction (XRD), Energy dispersive X-ray spectroscopy (EDX) and scanning electronic microscopy (SEM). The mineral phase of precipitated $CaCO_3$ was identified using X-ray diffractometer ((Bruker MeaSrv D2-208219, Germany-Central Lab, Faculty of science, Alexandria University) that operating with Cu Kα radiation (λ = 0.15406 nm) generated at 30 kV and 30 mA with scan rate of 2°/min for 2θ values

https://doi.org/10.5194/bg-2019-444
Preprint. Discussion started: 16 December 2019
© Author(s) 2019. CC BY 4.0 License.

over a wide range of Bragg angles $10° \leq 2\theta \leq 80$. The microchemical sample analysis was carried out using EDX analyzer combined with SEM (JEOL JSM 6360LA, Japan). The morphological characteristics of bacterial $CaCO_3$ was observed using SEM (JEOL JSM 6360LA, Japan – Advanced Technologies and New Materials Research Institute (ATNMRI) SRTA-City) at an accelerating voltage of 20 kV **(Silva-Castro et al., 2015).**

2.5. Study of the parameters associated with $CaCO_3$ precipitation

The correlation between $CaCO_3$ formation and the parametric changes in culture media during different growth phases of all strains under study were investigated. The parameters; bacterial count, NR activity, concentrations of NO_3^-, NO_2^-, pH, electrical conductivity (EC), and weight of precipitated $CaCO_3$ were screened at constant time intervals. Strains were inoculated on the media, which were reported formerly and incubated at 30°C both aerobically and anaerobically for 10 days. At each time interval (6 h), about 15 mL aliquot of the culture was drawn and subjected for analysis. Pour plate method was applied for assessing the bacterial count (CFU/ mL) on nutrient agar and incubated overnight at 30°C. The precipitated $CaCO_3$ was collected by centrifugation at 10.000 g for 15 min, washed with sterile distilled water, air dried and weighed. The supernatant was used to determine the rest of parameters, where, pH values were measured using a pH indicator (PB-10, Sartorius AG), while EC measured using electric conductivity meter (JENWAY- 4510). The concentrations of NO_3^- and NO_2^-, were measured according to the procedure followed by **APHA, (1999)**.

3. Results and Discussion:

3.1. Isolation and identification of bacteria

Among 17-screened bacterial isolates, three of them 71A, VIP and EM4 were selected based on their high NR activity. Then isolates were subjected for taxonomic identification and examination of carbonatogenesis process. The partial 16S rDNA sequences of 1127, 1025 and 800 bp of isolates 71A, VIP and EM4 exhibited 98.4, 97.2 and 99.8% DNA similarities with *Lysinibacillus sphaericus*, *Raoultella planticola* and *Streptomyces pluricolorescens*, respectively. Their 16S rDNA sequences were

https://doi.org/10.5194/bg-2019-444
Preprint. Discussion started: 16 December 2019
© Author(s) 2019. CC BY 4.0 License.

deposited in the GenBank under accession numbers MK936472 (71A), MK551748 (VIP) and KY964509 (EM4). Strain 71A is belonging to the phylum Firmicutes and family Bacillaceae. Whereas, the taxonomic affiliation of VIP and EM4 are belonging to phylum Proteobacteria, family Enterobacteriaceae and phylum Actinobacteria, family Actinomycetaceae, respectively. As pointed out by **Silva-Castro et al., (2015)**, members of Firmicutes phylum are the most predominant in MICCP process through ureolysis. Besides, **Talaiekhozani et al., (2014)** referred to the calcification potency of ureolytic *Proteus vulgaris* in concrete self-healing, which grouped in family Enterobacteriaceae. Additionally, some genera affiliated to Actinobacteria deposited $CaCO_3$ based on metabolizing nitrogenated organic substrates such as peptone and yeast extract **(Torres et al., 2013).** The phylogenetic tree of the selected strains was constructed by the Neighbour-joining (NJ) method as indicated in Fig. 1.

3.2. Nitrate Reductase activity (NR)

Actually, among 17 screened isolates, *L. sphaericus* (71A), *R. planticola* (VIP), and *S. pluricolorescens* (EM4) showed the maximum NR activity, after 24 h of incubation exhibiting 449, 534 and 768 µmole/ min/ml, respectively under aerobic conditions. However, under anaerobic conditions and on the 1st day of incubation, NR activity was 189 and 426 µmole/min/ml with strains 71A and VIP, respectively. In general, the NR activity of both strains was increased along with the incubation time as mentioned later on. On the other hand, strain EM4 did not show NR activity anaerobically, while it exhibited the highest NR activity aerobically. Therefore, it was selected. Our knowledge, there were no previous studies reported *Streptomyces* species in carbonatogenesis process through nitrate dissimilation pathway.

3.3. $CaCO_3$ biodeposition

Despite of almost preceding literature emphasized that the successes in isolation of CCP organisms are in particular based on the selection of sampling sites (calcareous and cementitious); the existing investigation did not comply with this rule. Despite, all of the isolates were isolated from non-calcareous sites; they possessed the specified mechanism, which allows $CaCO_3$ biodeposition

https://doi.org/10.5194/bg-2019-444
Preprint. Discussion started: 16 December 2019
© Author(s) 2019. CC BY 4.0 License.

(Montano-Salazar et al., 2017). The selected strains that precipitated crystals in CCP medium at 30°C under aerobic and anaerobic conditions exhibited different appearance, which includes crystal size, texture and color Fig. 2. Conversely, clear solution without any precipitates was observed in the abiotic uninoculated experiment (control), implying the ability of active strains to modify the chemistry of culture media and creating the proper microenvironments favoring $CaCO_3$ precipitation. Obviously, large beige or buff color and irregular crystals were appeared in anaerobic cultures, whereas fine white powder was formed in aerobic cultures of strains 71A and VIP, while, strain EM4 culture showed yellowish- brown aggregated pellets. Interestingly, the inter-species differences in crystallization patterns, colors, textures and forms were noticed previously by **Montano-Salazar et al., (2017)**, where, *Rhodococcus qingshengii* M101, *Arthrobacter crystalopoyetes* and *Psychrobacillus psycrodurans* showed spherical brown, irregular yellowish and irregular white/beige aggregated crystals of $CaCO_3$, respectively.

To study the involvement of nitrate dissimilation in $CaCO_3$ formation, the changes in the chemistry of media was monitored. Generally, a positive correlation was observed between the amount of precipitated $CaCO_3$ with bacterial growth that was synchronized with NR activity, pH, EC, NO_3^-/NO_2^- reduction Fig. 3. The aerobic growth resulted in the higher bacterial count, NR activity and eventually higher amount of $CaCO_3$. Such is plausible due to the availability of higher redox potential in presence of oxygen (+818 mV), which supports rapid energy generation, higher metabolic activity and hence higher reproduction rate **(Ilbert and Bonnefoy, 2013)**. Evidently, the cell number increased rapidly and reached to the maximum between 90h and 120h depending on the strain, thereafter it decreased slowly and steadily until the end of the experiment (240h). Remarkably, upon 120h of aerobic incubation, about 4.5x 10^8 CFU/mL of strain 71A with maximum NR activity (779 µmol/min/mL) completely reduced NO_3^- and uplifted pH from 7.01 to 8.53. In the same extent, the aerobic culture of strain VIP removed NO_3^- completely and elevating the initial pH from 7.01 to 8.91 at 90h by the activity of 6.65 x 10^8 CFU/ml, which exhibiting 862 µmol/min/mL of NR activity. Interestingly, strain EM4 (6.6 x 10^7 CFU/ ml) displayed the highest NR activity with 1292 µmol/min/mL and increasing pH to 9.51 with complete NO_3^- reduction at 102h of incubation.

https://doi.org/10.5194/bg-2019-444
Preprint. Discussion started: 16 December 2019
© Author(s) 2019. CC BY 4.0 License.

In comparison, the anaerobic cultures (9.7 x 10^6 and 7.1 x 10^7 CFU/ mL) of strains 71A and VIP eliminated NO_3^- by means of 180 and 66h, respectively. However, NR activity and pH were recorded 372 and 661 µmol/min/mL and 8.8 and 9.7 for 71A and VIP, respectively. In addition, a complete denitrification process was achieved upon continued anaerobic incubation. Obviously, NR activity was expressed aerobically even after the complete depletion of NO_3^- and in the presence of NO_2^-, whereas, under anaerobic conditions, it induced only in the presence of NO_3^-. That could be assigned to the physiological role differences of NRs under different aeration conditions**.** Remarkably, membrane-bound NR is induced under the absolute absence of oxygen and mainly involves in anaerobic nitrate respiration, for production of the electrochemical proton gradient and generation of ATP (**Zaki et al., 2019**). On the other hand, periplasmic NR is unaffected by oxygen level or C and N balance; it maintains redox homeostasis by dissipating excess reductant during aerobic growth and scavenging toxic concentrations of nitrate and nitrite as pointed out by **Li et al., (2012).** Thus, NR activity was observed along with aerobic incubation process. Furthermore, the availability of more bacterial cell number enables more nucleation sites, which ultimately precipitate more carbonate crystals **(Rodriguez-Navarro et al.2007).** Virtually, the amount of $CaCO_3$ precipitates kept increasing gradually during the mineralization process and recorded in g/100 mL, 3.27 and 1.55 for strain 71A (aerobic and anaerobic), 3.75 and 1.87 for strain VIP (aerobic and anaerobic) and 4.15 for strain EM4 (aerobic only), by 240h of incubation. On the other hand, **Gomaa, (2018)** stated that *Micrococcus* sp. induced 10.80 mg/ml of $CaCO_3$. Additionally, **Kaur et al., (2013)** documented that within three weeks of incubation, *B. megaterium, B. subtilis, B. thuringiensis, B. cereus* and *L. fusiformis* produced 187, 178, 167, 156 and 152 mg/100 ml of $CaCO_3$ via ureolysis pathway, which make results of the current study characteristic. Regarding the incubation time, a similar period for the $CaCO_3$ biodeposition was observed by **Rodriguez-Navarro et al. (2007)** for *Myxococcus xanthus***.**

Consistent with the bacterial count, NR activity and pH, a linear progressive increase in EC was noticed. That could be ascribed to the elevation of medium conductivity (mS/cm/min) by the action of charged ions such as NO_2^-, N_2O^-, NO^-, Ca^{2+} and CO_3^- ions generated by microbial activity on non-conductive substrates (sodium acetate and $Ca(NO_3)_2{\cdot}4H_2O$). It is worth mention that the conductimetric

https://doi.org/10.5194/bg-2019-444
Preprint. Discussion started: 16 December 2019
© Author(s) 2019. CC BY 4.0 License.

method is mainly used in evaluation of ureolysis process to follow the generation of ionic products from non-ionic substrates and consequently give insight on the microbial activity and mineralization tendency. Besides, it was used to control the kinetics of nucleation and crystal growth of carbonate precipitation process in the presence of exopolymer as referred by **Szcześ et al., (2018)**. Near the end of the experiment, a slight decline or stability state was observed by the almost of examined parameters for all bacterial strains both aerobically and anaerobically. That could be attributed either to entrance of the cells in stationary phase, where no more increase in cell number as a result of nutrient depletion and subsequently no more $CaCO_3$ precipitation, or fossilization of the cells within $CaCO_3$ crystals. The latter case caused mineralization of bacterial cell wall, which subsequently inhibited nutrient exchange with surrounding environment and eventually cell death as recorded by **Silva-Castro et al., (2015).**

3.4. $CaCO_3$ crystal analysis

XRD, EDX, and SEM techniques were employed to characterize the deposited $CaCO_3$ crystals. The nature of crystals, crystallographic identity and phase purity of inorganic compounds were determined using XRD. The characteristic signature peaks of calcite at 2θ values of 23.13, 29.50, 36.04, 39.51, 43.31, 47.51, 48.65, 56.71, 57.50, 60.81, 63.22, 64.42, and 65.57, respectively correlated with lattice (hkl) indices of (012), (104) (110), (113), (202), (024), (116), (211), (122), (214), (125), (300) and (0012) were identified in strain 71A precipitated samples under both incubation conditions. On the other hand, the XRD spectrum of strain VIP samples recorded calcite and vaterite under aerobic and anaerobic conditions, respectively Fig. 4. In regards to examined sample of strain EM4, the relative intensities and the reflection peak positions at 20.93, 24.81, 27.13, 32.75, 39.82, 42.66, 43.13, 49.85, 51.13, 55.75, 60.36, 62.54 and 65.38, which corresponds to crystallographic planes of (002), (100), (101), (102), (103), (004), (110), (104), (200), (202), (105), (114) and (006), respectively, confirms the presence of vaterite Fig. 4 (D & E). The diffraction peaks of calcite and vaterite match with those of the standard spectrum JCPDS, No. 02-0629 and. JCPDS, No. 72-0506, respectively **(Svenskaya et al., 2017).** Generally, the diffractograms of all examined samples appeared sharp,

https://doi.org/10.5194/bg-2019-444
Preprint. Discussion started: 16 December 2019
© Author(s) 2019. CC BY 4.0 License.

clearly distinguishable and broad, which indicates the pure, ultra-fine nature, small crystallite size and negating the possibility of mixed phases biominerals.

The EDX microanalysis of the bioprecipitated crystals ae presented in Fig. 5. The elemental profiles of the examined samples exhibited typical characteristic elemental peaks at 0.277, 0.525 and 3.69keV with atomic percentages range of (17-20 %), (42-51%), and (32-40%), which is related to the binding energies of carbon, oxygen and calcium, respectively. Additionally, there were other EDX peaks could be noticed in a small percentage such as Na and Cl, which proposed to be ingredients of culture media. This result is in agreement with **Han et al., (2018).** Obviously, vaterite samples of anaerobic culture of strains VIP and EM4 displayed another additional phosphorus (P) peak (2.013 keV) with considerable percentage assessed by 2-3%. Apparently, its presence could suggest being a biological origin, where, it represents essential constituent of bacterial biomolecules such as phospholipids, nucleic acids, proteins and/or polysaccharides. The involvement of vaterite with P is considered to be advantageous by providing stabilization and subsequently preventing transformation to calcite form. The same result was obtained with other research groups (**Ghosh et al., 2019)**. Generally, the calcium peaks intensities and their corresponding atomic percentages, which were higher than carbon peak, may reflect higher purity in structure as implied by **Caicedo-Pineda et al., (2018).**

The detailed characterization about the morphology, texture, surface and size of bio-deposited $CaCO_3$ crystals were studied by SEM. As shown in Figure 6A, approximately square or cubic shape $CaCO_3$ crystals in the range of 0.2 to 3.7 µm was noticed with strain 71A under aerobic condition. Close up view of these crystals depicted smooth surface embedded with rod shaped bacterial cells Fig. 6 (B) and some wrinkled surface globules with internal small holes Fig. 6 (B), indicated by arrows). Higher magnification in another sector displayed casts of bacterial cells and rhombohedral particles cemented in mucous matrix as referred by head arrow Fig. (6C), such mucilaginous like material could be considered as a polysaccharide excreted by carbonatogenic bacteria. This result concurred with the previous report in which rhombohedral calcite was produced by *B. megaterium* and embedded in slimy matrix **(Kaur et al., 2013).** On the other hand, the calcite formed anaerobically appeared as aggregated

https://doi.org/10.5194/bg-2019-444
Preprint. Discussion started: 16 December 2019
© Author(s) 2019. CC BY 4.0 License.

grains in size of 6.2 to 22.4 µm and irregular shaped clusters Fig. 6 (D). Additionally, subhedral rhombohedral particles with defined faces and edges were observed accompanying with anhedral crystals Fig. 6 (E). The presence of mucoid substance that encompassed these particles were also detected Fig. 6 (E), head arrows. Further, round shaped calcified bacterial cells were evident on the surface of bioliths Fig. 6 (F). Such change in cell morphology at anaerobic conditions could be ascribed to unfavorable conditions that lead to sporulation of vegetative cells. Virtually, the sporulation capability of strain 71A seemed to be advantageous; particularly in prospective applications with harsh conditions as self-healing of concrete cracks. In fact, bacterial spores are able to withstand adverse environmental conditions to maintain cell viability (**Vashisht et al., 2018).** However, the calcite mineralized by aerobic culture of strain VIP exhibited coarse, imbricated subhedral, rhombohedral minerals with size ranged from 0.79 µm to 1.63 µm Fig 6 (G). Viewed at higher magnification Fig 6 (H), the calcite crystals were accumulated compactly and assembled into stacks like structures. The bacterial cell contours were evident on calcite surface (indicated by arrows) Fig. 6 (I). Interestingly, calcite crystals with size range (1–10 µm) were produced during nitrate assimilation process by saprophytic fungus *Alternaria sp.* **(Hou et al., 2011),** which is consistent with results of the present study.

Remarkably, the vaterite of anaerobic strain VIP culture showed series of globules, spherulite crystals with size range of 12.3 to 61.8 µm Fig. 6 (J & K). In addition, the bacterial imprints were indicated by cavities on smooth surface of the sphere Fig. 6 (L). Such imprints emphasized the intrinsic role of bacterial cell as nucleation site for CaCO3 precipitation, which totally concurred with the finding of **Li et al., (2012)**. In coincident with our results, **Rodriguez-Navarro et al., (2012)** demonstrated the ability of *Myxococcus* sp. to induce different morphologies of both vaterite and calcite depending on growth conditions and medium composition. On the other hand, the spiny vaterite beads (5.5 – 77.6 µm), which spiked with triangular sharp point surface, were formed by strain EM4 Fig. 6 (M). The magnified field of vaterite pellets illustrated ramified CaCO3 crystals encapsulated the hyphae of *Streptomyces* cells Fig. 6 (N & O). Similar results were obtained with **Caicedo- Pineda et al., (2018)**. Otherwise,

https://doi.org/10.5194/bg-2019-444
Preprint. Discussion started: 16 December 2019
© Author(s) 2019. CC BY 4.0 License.

elongated plate-like crystals were produced by the actinomycete culture of *Thermomonospora* sp. **(Rautaray et al., 2004).**

Notably, the bacterial cells and their corresponding metabolic activity were prerequisite for the bioprecipitation of $CaCO_3$ crystals, particularly with absence of such deposition in abiotic negative control **(Han et al., 2017)**. Generally, the nitrate bioreduction is the predominant mechanism in $CaCO_3$ precipitations, which was summarized in the equation (1) to be followed by the strains under study **(Ivanov et al., 2015):**

$$5\ CH_3COONa + 4\ Ca(NO_3)_2 \rightarrow 4\ CaCo_3\downarrow + 4\ N_2\uparrow + 6\ CO_2\uparrow + 5\ H_2O + 5\ OH^- \quad \text{Eq. (1)}$$

In fact, the studied bacterial species reduced nitrate by NR enzymes to oxidize the organic carbon and electron donor (acetate) for energy generation and cells proliferation. As referred by **Singh et al., (2015)** and **Zhu and Dittrich, (2016),** protons were consumed continuously during such process and resulted in production of respired CO_2 and bicarbonate which ultimately elevated pH and alkalinity of ambient medium **(Hou et al., 2011; Zhu and Dittrich, 2016).** Under this circumstance, the precipitation/crystallization process is initiated in two main steps based on the crystal growth theory **(Trushina et al., 2014).** The first is crystal nucleation, which a new solid phase in nanometer size forms in supersaturated solution **(Wu et al., 2017)**. The second step is crystal growth, which could be described as atom-by-atom addition to the newly formed nuclei. Consequently, the growth of larger crystals and increasing in the particles size either occur randomly or oriented at the expense of smaller crystals or nanoaggregates **(Zhou et al., 2010).** The particles with lower surface charge tend to coagulate and agglomerate to each other in a crystallographically oriented manner till reach to the most stable crystals with particular size that cause sedimentation. Thus, at this point the precipitation process is completed **(Rodriguez-Navarro et al. 2007; Trushina et al., 2014)**. Substantially, such precipitation process is not genetically or biologically controlled by the microorganism itself, but mediated by the physico-chemical properties of the surrounding environment (**Caicedo-Pineda et al., 2018**).

https://doi.org/10.5194/bg-2019-444
Preprint. Discussion started: 16 December 2019
© Author(s) 2019. CC BY 4.0 License.

Noteworthy in this context is nucleation of crystals and solution supersaturation, which determine the size and polymorphic form of precipitated crystals **(Vekilov, 2010).** Where, crystal nucleation dominates over crystal growth at a relatively higher degree of supersaturation, which ultimately generates smaller size with approximately identical shaped crystals. On the other hand, at low supersaturation, the nucleation is slow and crystals grow faster than they do nucleate, resulting in aggregates of large crystals of various sizes forms **(Rodriguez-Navarro et al. 2007; Wu et al., 2017).** Such principle could explain the formation of small size deposits at aerobic cultures. In addition, it was suggested that anaerobic cultures of strains 71A and VIP excreted certain polysaccharides with adhesive nature that stickled tightly the fine particles into larger crystals. In agreement with these results, **Shirakawa et al., (2011)** stated that under static conditions, culture of *L. sphaericus* precipitated larger $CaCO_3$ crystals than in shaken cultures.

In the same extent, as pointed out by **Rodriguez-Blanco et al., (2017)**, the structure, morphology, stability and crystallization pathway of $CaCO_3$ precursor to either vaterite or calcite governorates by several factors. These include binding strength of Ca^{2+} and CO_3^{2-} ions within the $CaCO_3$ precursor aggregates, solubility, and the dissolution rate of $CaCO_3$ precursor, which all are pH-dependent. It is substantial to mention that alternation in pH values contributes in the ionic strength, which consequently effects on solution saturation. Where, higher supersaturation occurs at higher pH, alkalinity and carbonate ions concentrations. In addition, at higher supersaturation, the crystals with higher solubility and lower stability form first and vice versa as described by the Ostwald's law of stages **(Rodriguez-Navarro et al. 2007; Trushina et al., 2014).** That could explain vaterite formation by anaerobic culture of strain VIP and strain EM4; where higher metabolic activity accompanying with nitrate dissimilation process led to increase carbonate content and rapidly elevating pH values 9.58 (VIP) and 9.7 (EM4) to the point of supersaturation with respect to vaterite. On the other hand, under relatively low supersaturation, calcite formed by aerobic culture of strain VIP, aerobic and anaerobic cultures of strain 71A at pH 8.9, 8.5, and 8.78, respectively. As pointed out by **Rodriguez-Navarro et al., (2012)**, the formation of vaterite and calcite were promoted at alkaline (8.5-10.5) and neutral pH (7), respectively. On contrary, **Rautaray et al., (2004)** stated that synthesis of vaterite by *Verticillium sp.* was facilitated

https://doi.org/10.5194/bg-2019-444
Preprint. Discussion started: 16 December 2019
© Author(s) 2019. CC BY 4.0 License.

at low pH conditions (5.3), whereas calcite is favorably formed at pH more than 10 **(Ramakrishna et al., 2016).**

Besides pH, there are several key factors governed the type, crystal size and polymorph of the biodeposited crystals including; bacterial type, nucleation sites abundance, calcium concentrations, calcium precursor type, media composition and incubation conditions **(Anbu, et al., 2016; Chaparro-Acuña et al., 2018)**. Accordingly, the bacterial species was considered being the MICCP determinant in the current study. Therefore, it is plausible to mention that bacterial surfaces properties could also influence greatly on phase and morphology of $CaCO_3$ through heterogeneous nucleation. It is promoted by coupling and binding of negatively charged functional (macro) molecules in the bacterial cell wall and positively charged cations (e.g. Ca^{2+}). In general, the bacterial cell wall consists of peptidoglycans, teichoic lipoteichoic acids, lipids and lipopolysaccharide, which provide the negative charge of cell wall. As reported by **Anbu, et al., (2016),** Ca 2+ ions prevented from accumulation inside the cell and adsorbed more frequently on cell envelope due to potency of the cell for ionic selectivity. Thereby, Ca 2+ ions were actively transferred out through passive diffusion by the action of an ATP-dependent pump which is located close to outside of the cell. With continuous H+ uptake, higher Ca2+ concentration and higher pH are emerged surrounding the cell, creating nanoscale neighborhood that facilitate precipitation and crystal growth of CaCO3 as described in equations 2, 3 and 4 (Li et al., 2011; Singh, 2019):

$$Ca^{+2} + cell^{-} \rightarrow Cell\text{-}Ca^{+2} \qquad \text{Eq. (2)}$$

$$HCO_3^{-} \leftrightarrow H^{+} + CO_3^{-2} \qquad \text{Eq. (3)}$$

$$Cell\text{-}Ca^{+2} + CO_3^{-2} \rightarrow Cell\text{-}CaCO_3\downarrow \qquad \text{Eq. (4)}$$

Remarkably, heterogeneous nucleation is commonly occurred process in nature **(González-Muñoz et al., 2014)**. Furthermore, other bacterial components such as lipids, glycoproteins, proteins, proteoglycans and extracellular polymeric substances (EPS) could provide additional nucleation site for $CaCO_3$ precipitation during carbonatogenesis process **(Li et al., 2011; Ghosh et al., 2019).** Such

https://doi.org/10.5194/bg-2019-444
Preprint. Discussion started: 16 December 2019
© Author(s) 2019. CC BY 4.0 License.

organic macromolecules are acidic polyanionic polymers which include carboxylic ($R\text{-}COO^-$), phosphatic ($R\text{-}PO_4^{2-}$) or sulfonate ($R\text{-}SO_3^-$) functional groups, and can serve as promoters or inhibitors for crystals biomineralization **(Szcześ et al., 2018).**

Actually, when charged functional groups of EPS exist in a random distribution, they couple to metals in a disordered arrangement, which obstruct crystal nucleation. However, the presence of EPS functional groups in periodic and ordered array lead to stereo chemical gathering between the organic matrix and the newly-formed crystals and hence promotes heterogeneous nucleation **(González-Muñoz et al., 2014).**

Virtually, the culture of strain VIP might exhibit different metabolic products, proteins or EPS under different aeration conditions, which thereafter affected on the kinetics of crystallization process. Where, the biomolecules under certain condition may exhibit great affinity to certain face of specific polymorph and will adsorb onto these faces, causing alterations in crystals nucleation or growth stages of the affected polymorph on the account of the others **(Trushina et al., 2014).** Notably, EDX analysis Fig. 4 (D & E) elucidated the incorporation of phosphorus peak with precipitated vaterite of both EM4 and anaerobic culture of VIP strains. That could explain the stability of such metastable phase and inhibition of its conversion to stable phase (aragonite or calcite). Such biologically originated phosphorus exhibits certain affinity to Ca^{2+}. As it preferentially complexes with crystal nucleus and adsorbs on specific site during crystal growth causing growth inhibition; generating metastable vaterite **(Trushina et al., 2014).** It is noteworthy to mention that *Streptomyces* cell wall contain teichoic, which contains 1, 5-poly (ribitol phosphate) chain along with poly (glycerol phosphate) unites linked together by phosphodiester bonds **(Streshinskaya et al., 2003).** Besides, it also contains diamino acid, LL-diaminopimelic acid accompanied by glycine (**Nakamura et al., 1977),** which eventually confirm vaterite stabilization. Several literatures documented that the preservation of bio-vaterite was favored by organophosphorous biomolecules or phosphorus-enriched medium (**Caicedo-Pineda et al., 2018).**

Interestingly, **Tourney and Ngwenya, (2009)** shed the light on the dissolved organic carbon, which liberated from EPS and bound with Ca^{2+} ions, causing lowering of $CaCO_3$ saturation which

https://doi.org/10.5194/bg-2019-444
Preprint. Discussion started: 16 December 2019
© Author(s) 2019. CC BY 4.0 License.

consequently enhances calcite precipitation over vaterite. Additionally, **Kawaguchi and Decho, (2002)** declared that the association of specific proteins with EPS of *Schizothrix sp.* favored aragonite and calcite polymorph selection. In the same sense, extracellular proteins excreted by the *Verticillium sp.* and *Thermomonospora sp.* influenced significantly on both crystal morphology and polymorph selectivity as refereed by **Rautaray et al., (2004**).

However, it was recorded that the appropriate nutrient types (e.g. carbon/ energy source and nitrogen source) and their concentrations stimulate the bacterial growth rate and enzymatic system, and thus provide the required chemical species and appropriate conditions for precipitation **(Kaur et al., 2013).** Alternatively, the different calcium sources induce different mineral shape and polymorph **(Anbu, et al., 2016; Kim et al., 2016; Chaparro-Acuña et al., 2018).** Where, rhombohedral calcite and disk-shaped vaterite were induced by calcium chloride and calcium acetate, respectively. While, spherical shape vaterite was induced by calcium lactate and calcium gluconate **(Anbu, et al., 2016).**

Herein, despite acetate and calcium nitrate supported good growth and rapid metabolic activity for examined bacteria, but these factors had no effect on polymorphic selectivity of $CaCO_3$ minerals as it was fixed with all examined bacterial species. In correspondence with current study, **Rothenstein et al., (2012)** reported that Ca-acetate in the culture media of *Halomonas halophila* displayed no effect on the mineralized polymorph. Apparently, the current study has obviously shown that the variation in size, morphology and mineral phase of the biodeposited mineral is driven by strain-specific differences. Generally, the calcite/vaterite selectivity is a complex process and controversial issue **(Rodriguez-Navarro et al. 2007; González-Muñoz et al., 2014).**

The studies on the formation of spherical vaterite crystals in synthetic systems are relatively scarce (**Rautaray et al., 2004**, **Rodriguez-Blanco et al., 2017)**. Actually, different problems encountered during synthesis, crystallization and stabilization. In particular with its instability and rapidly transformation into more stable phases (calcite or aragonite) at room temperature, and in an aqueous solution. Besides, the reproducibility and shape/size control of vaterite are taken in consideration. To overcome the above-mentioned concerns, certain additives either organic or inorganic were applied.

https://doi.org/10.5194/bg-2019-444
Preprint. Discussion started: 16 December 2019
© Author(s) 2019. CC BY 4.0 License.

Nitric acid and ammonia are among inorganic additives, which deemed as facilitating factors influence on the kinetics of vaterite production **(Trushina et al., 2014).** However, polymers such as, polyacrylic acid, poly (vinyl alcohol), polycarboxylic acid, polyvinylpyrrolidone and commercial copolymers; including poly (4-styrenesulfonate-co-maleic acid) (PSS-co-MA), calixarene dendrimers were the most frequently used. Moreover, different types of alcohols and some ionic surfactant were utilized as an effective stabilizing and polymorph controlling agents **(Trushina et al., 2014).** The traces of such compounds associated with vaterite particles could exhibit undesired impact especially in applying vaterite in drug delivery and pharmaceutical formulations. Thus, all the sights directed to use biomimetically synthesized substances such as gelatin **(Wu et al., 2017),** Chitosan **(Wu et al., 2011),** amino acids and proteins **(Trushina et al., 2014).**

Nonetheless, the natural and biological matter is even better as documented by **Wu et al., (2017).** Where, the carbonatogenic bacteria of the current study serve as a source of carbonate ions makes this a truly biogenic approach for minerals synthesis; hence does not consider merely biomimetic process. Actually, the carbon dioxide utilized in biomineralization generated from metabolism of carbonatogenic bacteria themselves and was not provided by external source as reported in other biomimetic studies **(Rautaray et al., 2003; Han et al., 2018**). In the same manner, **Hou and co-workers, (2011)** found that the nitrate uptake by *Alternaria* sp. caused of $CaCO_3$ formation via sequestration of respiratory CO_2 and thus reduce its emission and indirectly diminishing the rate of global warming.

Finally, the total biological synthesis of calcite and vaterite crystals under nitrate dissimilation conditions by strains 71A, VIP, and EM4 has not been reported previously. These carbonatogenic bacteria with their implications in crystal engineering open up the possibility to various prospective applications include; bioremediation of building stone, monuments/statuary, consolidation/strengthening of soil/sand, the reduction of the porosity and permeability of geological formations. Besides, the characteristic features of vaterite [the biocompatibility, biosafety, biodegradability, high (solubility, porosity, specific surface area), dispersion, accessibility and pH-sensitivity properties of $CaCO_3$] make it highly appealing in biomedicine applications such as

https://doi.org/10.5194/bg-2019-444
Preprint. Discussion started: 16 December 2019
© Author(s) 2019. CC BY 4.0 License.

bone/teeth implants, sensor applications and drug delivery **(Rautaray et al., 2004; Poelvoorde, 2017)**. Additionally, the overall carbonatogenic process would be utilized in softening of hard water and CO_2 capturing from atmosphere and wastewater treatment systems in prospective studies.

4. Conclusion

In conclusion, for the first time the present study demonstrated that the bacterial strains *L. sphaericus* (71A), *R. planticola* (VIP), and *S. pluricolorescens* (EM4) isolated from Egyptian non-calcareous niches, induced carbonatogenesis process through nitrate reduction under aerobic and anaerobic conditions. XRD, EDX and SEM techniques were used to characterize precipitated $CaCO_3$, which found to differ in their properties according to the type of strain as well as growth conditions. Precipitated $CaCO_3$ was either calcite or vaterite. Overall, carbonatogenesis process via nitrate reduction is totally biological, ecofriendly, inexpensive, and promotes $CaCO_3$ precipitations without accumulation of toxic by-product such as ammonia.

Data availability. The data of this study are available for public after a request to the corresponding author

Author contributions. The authors ME, SZ and DA contributed to plan of the wok, results explanation manuscript writing and data analysis. AK helped in the practical part.

Competing interests. The authors declare that they have no conflict of interest.

Acknowledgment

This research was conducted at Genetic Engineering and Biotechnology Research Institute, City of Scientific Research and Technological Applications, Burgelarab city, Alexandria, Egypt

Financial support. This research did not receive any specific grant from funding agencies in the public, commercial, or not-for-profit sectors.

https://doi.org/10.5194/bg-2019-444
Preprint. Discussion started: 16 December 2019
© Author(s) 2019. CC BY 4.0 License.

References

Anbu, P., Kang, C., Shin, Y., and So, J.: Formations of calcium carbonate minerals by bacteria and its multiple applications. Springer Plus, 5, 250, doi: 10.1186/s40064-016-1869-2, 2016.

Caicedo-Pineda, G.A., Prada-Fonseca, M.C., Casas-Botero, A.E., and Martínez-Tejada, H.V.: Effect of the tryptone concentration on the calcium carbonate biomineralization mediated by *Bacillus cereus*, DYNA, 85, 69-75, http://dx.doi.org/10.15446/dyna.v85n205.60637. 2018

Chaparro-Acuña, SP., Becerra-Jiménez, ML., Martínez-Zambrano, JJ., and Rojas-Sarmiento, HA.: Soil bacteria that precipitate calcium carbonate: mechanism and applications of the process, Acta. Agron., 67, 277-288, DOI: 10.15446/acag.v67n2.66109. 2018

Ersan, Y., Belieb, N., and Boon, N.: Microbially induced $CaCO_3$ precipitation through denitrification: Anoptimization study in minimal nutrient environment, Biochem. Engin. J., 101, 108–118, http://dx.doi.org/10.1016%2Fj.bej.2015.05.006. 2015

Ghosh, T., BhaduriI, S., Montemagno, C., and Kumar, A.: *Sporosarcina pasteurii* can form nanoscale calcium carbonate crystals on cell surface, Plosone, 14, 1, doi: 10.1371/journal.pone.0210339. 2019

GOMAA, E.Z.: Biosequestration of heavy metals by microbially induced calcite precipitation of ureolytic bacteria, Roman. Biotechnol. Letters X, 1-11, https://www.rombio.eu/docs/Biosequestration%20of%20heavy%20metals%20by%20microbially%20induced%20calcite%20precipitation%20of%20ureolytic%20bacteria.pdf. 2018.

González-Muñoz, M. T., Rodriguez-Navarro, C., Martínez-Ruiz, F., Arias, J. M., Merroun, M. L., and Rodriguez-Gallego, M.: Bacterial biomineralization: new insights from *Myxococcus*-induced mineral precipitation, Geological Society, London, Special Publications, 336, 31-50. 2014

Han, Z., Li, D., Zhao, H., Yan, H., and Li, P.: Precipitation of Carbonate Minerals Induced by the Halophilic Chromohalobacter Israelensis under High Salt Concentrations: Implications for Natural Environments, Minerals, 7, 95, https://doi.org/10.3390/min7060095. 2018

Hou, W., Lian, B., and Zhang, X.: CO2 mineralization induced by fungal nitrate assimilation, Bioresour. Technol., 102, 1562–1566, doi: 10.1016/j.biortech.2010.08.080. 2011

© Author(s) 2019. CC BY 4.0 License.

529 Hu, Q., Zhang, J., Teng, H., and Becker, U.: Growth process and crystallographic properties of
530 ammonia-induced vaterite. American Mineralogist, 97, 1437–1445,
531 https://doi.org/10.2138/am.2012.3983. 2012
532 Ilbert, M., and Bonnefoy, V.: Insight into the evolution of the iron oxidation pathways, Biochimica et
533 Biophysica Acta, 1827, 161–175,
534 https://www.academia.edu/27856931/Insight_into_the_evolution_of_the_iron_oxidation_pathways.
535 2013
536 Ivanov, V., Chu, J., and Stabnikov, V.: Chapter 2: Basics of Construction Microbial Biotechnology,
537 Springer International Publishing Switzerland, F. Pacheco Torgal et al. (eds.), Biotechnologies and
538 Biomimetics for Civil Engineering, http://dx.doi.org/10.10071/2015. 2015
539 Kaur, D. N., Reddy, M. S., and Mukherjee, A.: Biomineralization of Calcium Carbonate Polymorphs by
540 the Bacterial Strains Isolated from Calcareous Sites, J. Microbiol. Biotechnol., 23, 707–714,
541 https://www.ncbi.nlm.nih.gov/pubmed/23648862. 2013
542 Kawaguchi T, and Decho, AW.: A laboratory investigation of cyanobacterial extracellular polymeric
543 secretions (EPS) in influencing $CaCO_3$ polymorphism, J. Cryst. Growth, 240, 230-235,
544 https://www.researchgate.net/publication/228593393. 2002
545 Kim H., Hyo, J., Chulwoo, P., Jaejoon, J., Bora, S., Wook, K., Namhyun, C., In-Geol, C., and Woojun,
546 P.: Calcium Carbonate Precipitation by Bacillus and Sporosarcina Strains Isolated from Concrete and
547 Analysis of the Bacterial Community of Concrete, J. Microbiol. Biotechnol., 26, 540–548,
548 http://dx.doi.org/10.4014/jmb.1511.11008. 2016
549 Li, W., Liu, L., Zhou, P., Cao, L., Yu, L., and Jiang, S.: Calcite precipitation induced by bacteria and
550 bacterially produced carbonic anhydrase, Curr. Sci., 100, 502-508,
551 https://www.currentscience.ac.in/Volumes/100/04/0502.pdf. 2012
552 Lin, Y.C., Turchyn, A.V., Steiner, Z., Bots, P., Lampronti, G.I., and Tosca, N.J.: The role of microbial
553 sulfate reduction in calcium carbonate polymorph selection, Geochimica et Cosmochimica Acta, 237,
554 184-204. https://doi.org/10.1016/j.gca.2018.06.019. 2018

© Author(s) 2019. CC BY 4.0 License.

555 Lv, P., Luo, J., Zhuang, X., Zhang, D., Huang,Z. and Bai, Z.: Diversity of culturable aerobic
556 denitrifying bacteria in the sediment. Water and biofilms in Liangshui River of Beijing, China,
557 Scientific reports 10032, 1-12. https://www.nature.com/articles/s41598-017-09556-9.pdf. 2017
558 Montano-Salazar, SM., Lizarazo-Marriaga, J., and Brandao, FBP.: Isolation and Potential
559 Biocementation of Calcite Precipitation Inducing Bacteria from Colombian Buildings, Curr. Microbiol.,
560 75, 256-265, doi: 10.1007/s00284-017-1373-0. 2017
561 Nakamura, T., Tamura, G., and Arima, K.: Peptidoglycan of Cell Wall of *Streptomyces*
562 *roseochromogenes*, Agricul. Biolog. Chem., 41, 763-768, https://doi.org/10.1271/bbb1961.41.763. 1977
563 O'Donnell, S., Rittmann, B., and Kavazanjian, E.: Factors Controlling Microbially Induced
564 Desaturation and Precipitation (MIDP) via Denitrification during Continuous Flow, Geomicrobiol. J.,
565 36, 543-558, https://asu.pure.elsevier.com/en/publications/factors-controlling-microbially-induced-
566 desaturation-and-precipit. 2019
567 Poelvoorde, L.: Calcium carbonate-based particles and capsules for therapeutic enzymes. Masterproef
568 voorgelegd voor het behalen van de graad master in de richting Master of Science in de industriële
569 wetenschappen, biochemie, https://www.scriptiebank.be/sites/default/files/thesis/2017-
570 09/Van%20Poelvoorde_2017.pdf. 2017
571 Ramakrishna, C., Thenepalli, T., Huh, J., and Ahn, J.W.: Precipitated calcium carbonate synthesis by
572 simultaneous injection to produce nano whisker aragonite, J. Korean Ceram. Soc., 53, 222–226,
573 doi:10.4191/kcers.2016. 53.2.222. 2016
574 Rautaray, D., Ahmad, A., and Sastry, M.: Biosynthesis of $CaCO_3$ Crystals of Complex Morphology
575 Using a Fungus and an Actinomycete, J. Am. Chem. Soc., 3, 14656-14657, DOI: 10.1021/ja0374877.
576 2004
577 Richardson, A., Coventry, K., Forster, A., and Jamison, C.: Surface consolidation of natural stone
578 materials using microbial induced calcite precipitation, Structural Survey, 32, 265-278,
579 https://doi.org/10.1108/SS-07-2013-0028. 2014
580 Rodriguez-Blanco, J.D., Sand, K.K., and Benning, L.G.: ACC and Vaterite as Intermediates in the
581 Solution-Based Crystallization of $CaCO_3$, Chapter 5, *New Perspectives on Mineral Nucleation and*

© Author(s) 2019. CC BY 4.0 License.

growth, Springer International Publishing Switzerland, DOI: 10.1007/978-3-319-45669-0; eBook ISBN: 978-3-319-45669-0. 2017

Rodriguez-Navarro, C., Jimenez-Lopez, C., Rodriguez-Navarro, A., Gonzalez-Mun˜oz, M., and Rodriguez-Gallego, M.: Bacterially mediated mineralization of vaterite, Geochim. Cosmochim. Acta, 71, 1197–1213, https://www.academia.edu/14655513/Bacteriallymediated_mineralization_of_vaterite. 2007

Rodriguez-Navarro, C., Jroundi, F., Schiro, M., ncarnación Ruiz-Agudo, E., and González-Muñoz, M.: Influence of Substrate Mineralogy on Bacterial Mineralization of Calcium Carbonate: Implications for Stone Conservation, Appl. Environ. Microbiol., 78, 4017–4029, https://dx.doi.org/10.1128%2FAEM.07044-11. 2012

Rothenstein, D., Johannes, B., Thomas Schreiber, D., Vera B., and Joachim, B.: Influence of zinc on the calcium carbonate biomineralization of Halomonas halophile, Aquatic Biosystems, 31, 1-13, http://www.aquaticbiosystems.org/content/8/1/31. 2012

Sevcık, R., Sasek, P., and Viani, A.: Physical and nanomechanical properties of the synthetic anhydrous crystalline $CaCO_3$ polymorphs: vaterite, aragonite and calcite, J. Mater. Sci., 53, 4022–4033, DOI: 10.1007/s10853-017-1884-x. 2018

Shirakawa, M.A., Cincotto, M.A., Atencio, D., Gaylarde, C.C., and John, V.M.: Effect of culture medium on biocalcification by *pseudomonas putida*, *lysinibacillus sphaericus* and *bacillus subtilis*, Brazil. J. Microbiol., 42, 499-507, doi: 10.1590/S1517-838220110002000014. 2011

Silva-Castro, G.A., Uad, I., Gonzalez-Martinez, A., Rivadeneyra, A., Gonzalez-Lopez, J.M., and Rivadeneyra, A.: Bioprecipitation of Calcium Carbonate Crystals by Bacteria Isolated from Saline Environments Grown in Culture Media Amended with Seawater and Real Brine, BioMed. Res. Int., 816102. https://dx.doi.org/10.1155%2F2015%2F816102. 2015

Singh, M.: Urease activity and deposition of calcium carbonate layers on a 16th century Mughal monument, Current Sci., 116, 1840- 1849, DOI: 10.18520/cs/v116/i11/1840-1849. 2019

Standard Methods for the Examination of Water and Wastewater, American Public Health Association (APHA, 1999): American Water Works Association- Water Environment Federation.

© Author(s) 2019. CC BY 4.0 License.

https://www.scirp.org/(S(lz5mqp453edsnp55rrgjct55))/reference/ReferencesPapers.aspx?ReferenceID=1909322. 1999

Streshinskaya, G. M., Kozlova, Yu. I., Shashkov, A. S., Evtushenko, L. I., and Naumova, I. B.: The Cell Wall Teichoic Acids of Streptomycetes from the "*Streptomyces cyaneus*" Cluster, Microbiol., 72, 455–460, https://link.springer.com/article/10.1023/A:1025048807873. 2003

Svenskaya, Y.I., Fattah, H., Inozemtseva, O.A., Ivanova, A.G., Shtykov, S.N., Gorin, D.A., and Parakhonskiy, B. V.: Key Parameters for Size- and Shape-Controlled Synthesis of Vaterite Particles, Crystal Growth Design, 1, 331-337, https://doi.org/10.1021/acs.cgd.7b01328. 2017

Szcześ, A., Czemierska, M., Jarosz-Wilkołazka, A., Magierek, E., Chibowski, E., and Hołysz, L.; Extracellular polymeric substance of Rhodococcus opacus bacteria effects on calcium carbonate formation, Physicochem. Probl. Miner. Process., 54, 142 150, https://doi.org/10.5277/ppmp1835. 2018

Talaiekhozani, A., Keyvanfar, A., Andalib, R., Samadi, M., Shafaghat, A., Kamyab, H., Abd Majid, M.Z., Zin, M. R., Fulazzaky, M. A., Lee, C. T., and Hussin, M. W.: Application of Proteus mirabilis and Proteus vulgaris mixture to design self-healing concrete, Desalin. Water Treat., 52, 3623–3630, https://www.academia.edu/7700659/Application_of_Proteus_mirabilis_and_Proteus_vulgaris_mixture_to_design_self-healing_concrete. 2014

Thirumalai, K.: Isolation and characterization of naturally occurring calcite-forming bacteria in Malaysia, Msc. lee kong chian faculty of engineering and science, universiti tunku abdul Rahman, http://eprints.utar.edu.my/1912/1/MSc-2015-0909188-01.pdf. 2015

Torres, A. R., Martinez-Toledo, M. V., Gonzalez-Martinez, A., Gonzalez-Lopez, J., Martı´n-Ramos, D., and Rivadeneyra, M. A.: Precipitation of carbonates by bacteria isolated from wastewater samples collected in a conventional wastewater treatment plant, Int. J. Environ. Sci. Technol., 10, 141–150, http://www.bioline.org.br/pdf?st13016. 2013

Tourney, J., and Ngwenya, B. T.: Bacterial extracellular polymeric substances (EPS) mediate $CaCO_3$ morphology and polymorph, Chem. Geol., 262, 138-146, DOI: 10.1016/j.chemgeo.2009.01.006. 2009

© Author(s) 2019. CC BY 4.0 License.

634 Trushina, D.B., Bukreeva, T.V., Kovalchuk, M.V., and Antipina, M.N.: $CaCO_3$ vaterite microparticles
635 for biomedical and personal care applications, Materials Sci. Engin., C 45, 644–658,
636 http://dx.doi.org/10.1016/j.msec.2014.04.050. 2014
637 Vashisht, R., Attrib, S., Sharmab, D., Shuklaa, A., and Goel, G.: Monitoring biocalcification potential
638 of Lysinibacillus sp. isolated from alluvial soils for improved compressive strength of concrete,
639 Microbiological Research, 207, 226–231, doi: 10.1016/j.micres.2017.12.010. 2018
640 Vekilov, P.G.: Nucleation, Crystal Growth & Design, 15, 5007–5019,
641 https://doi.org/10.1021/cg1011633. 2010
642 Wu, S., Chiang, C.Y., and Zhou, W.: Formation Mechanism of $CaCO_3$ Spherulites in the Myostracum
643 Layer of Limpet Shells, Crystals, 7, 1-15, https://doi.org/10.3390/cryst7100319. 2017
644 Zaki, S., Eltarahony, M., and Abd-El-Haleem, D.: Disinfection of water and wastewater by
645 biosynthesized magnetite and zerovalent iron nanoparticles via NAP-NAR enzymes of Proteus mirabilis
646 10B, Environ. Sci. Pollut. Res. Inter., 26, 23661-23678, doi: 10.1007/s11356-019-05479-2. 2019
647 Zhou, G., Yao, Q., fu, S., and guan, Y.: Controlled crystallization of unstable vaterite with distinct
648 morphologies and their polymorphic transition to stable calcite, Eur. J. Mineral., 22, 259–269, DOI:
649 10.1127/0935-1221/2009/0022-2008. 2010
650 Zhu, T., and Dittrich M.: Carbonate Precipitation through Microbial Activities in Natural Environment
651 and Their Potential in Biotechnology: A Review, Front Bioeng. Biotechnol., 4, 1-21,
652 https://dx.doi.org/10.3389%2Ffbioe.2016.00004. 2016
653
654
655
656
657
658

https://doi.org/10.5194/bg-2019-444
Preprint. Discussion started: 16 December 2019
© Author(s) 2019. CC BY 4.0 License.

659 **Figures legends**

660 **Figure 1:** Neighbour-joining phylogenetic tree based on 16S rDNA gene sequences, illustrating the
661 relationships between carbonatogenic strains 71A, VIP and EM4 and related species retrieved from
662 NCBI GenBank, their accession numbers are shown in parentheses. The bootstrap values above 50%,
663 expressed as percentages of 1000 replications are indicated at the branch points.

664 **Figure 2:** The morphological differences of calcium carbonate crystals precipitated by carbonatogenic
665 strains in liquid CCP media; A)-aerobic culture of strain 71A, B)-anaerobic culture of strain 71A, C)-
666 aerobic culture of strain VIP, D)- anaerobic culture of strain VIP, E)- aerobic culture of strain EM4; F,
667 G, H, I and K the air dried crystals with the same previous order.

668 **Figure 3:** Dynamic analysis of carbonatogenesis process associated with changes of pH, NO_3^-
669 concentration, NO_2^- concentration, cell growth, NR activity, EC and $CaCO_3$ weight, mediated by A)-
670 aerobic culture of strain 71A, B)- anaerobic culture of strain 71A, C)- aerobic culture of strain VIP, D)-
671 anaerobic culture of strain VIP and E)-aerobic culture of strain EM4. The average of three replica were
672 performed for each one. To adjust the scale, some parameters are multiplied and/or divided as indicated
673 on the figures.

674 **Figure 4:** XRD profile of $CaCO_3$ precipitated by A)- aerobic culture of 71A, B)-anaerobic culture of
675 71A, C)- aerobic culture of VIP, D)- anaerobic culture of VIP and E)- EM4 culture.

676 **Figure 5:** EDX crystallographic pattern of $CaCO_3$ precipitated by A)- aerobic culture of 71A, B)-
677 anaerobic culture of 71A, C)- aerobic culture of VIP, D)- anaerobic culture of VIP and E)- EM4 culture.

678 **Figure 6:** SEM micrographs of $CaCO_3$ crystal formed by nitrate reducing strains. A, B, C)- crystals
679 from aerobic culture of 71A, D, E, F)- crystals from anaerobic culture of 71A, G, H, I)- crystals from
680 aerobic culture of VIP, J, K, L)- crystals from anaerobic culture of VIP and M, N, O)- crystals from
681 EM4 culture.

682

683

https://doi.org/10.5194/bg-2019-444
Preprint. Discussion started: 16 December 2019
© Author(s) 2019. CC BY 4.0 License.

684

685

686

687

688

689

690

691

692

693

694

695

696

697

698

699

700

701

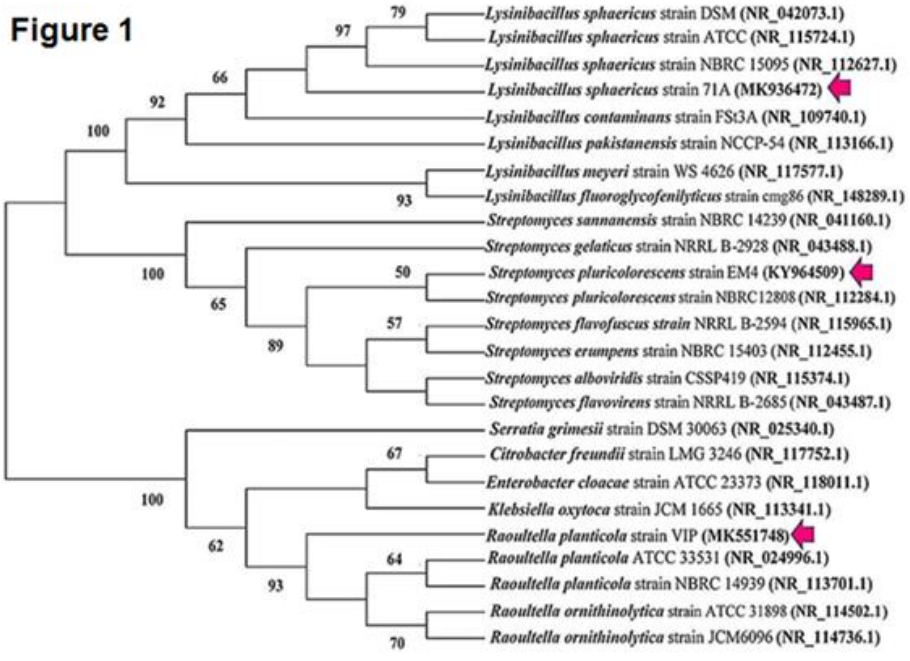

https://doi.org/10.5194/bg-2019-444
Preprint. Discussion started: 16 December 2019
© Author(s) 2019. CC BY 4.0 License.

Biogeosciences
Discussions
Open Access
EGU

702

703

Figure 2

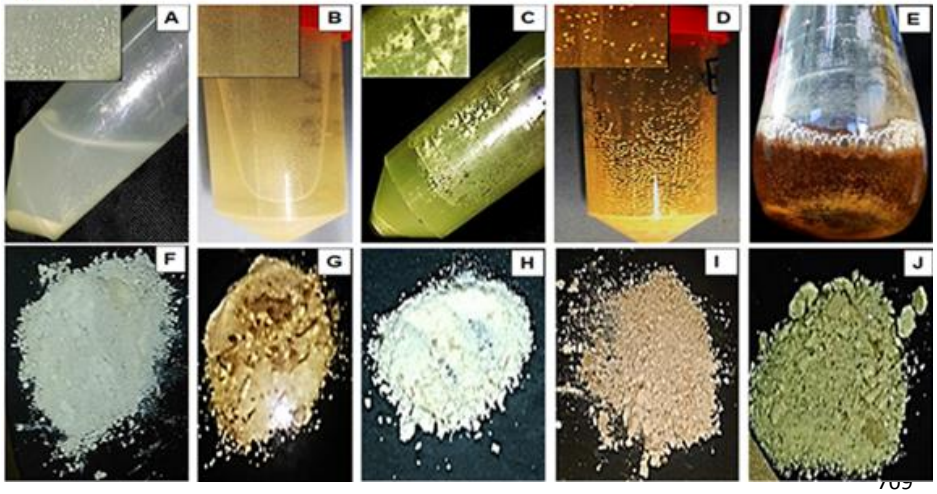

709

710

711

712

713

714

715

716

717

718

719

https://doi.org/10.5194/bg-2019-444
Preprint. Discussion started: 16 December 2019
© Author(s) 2019. CC BY 4.0 License.

Biogeosciences
Discussions
Open Access
EGU

720

721

Figure 3

722

723

724

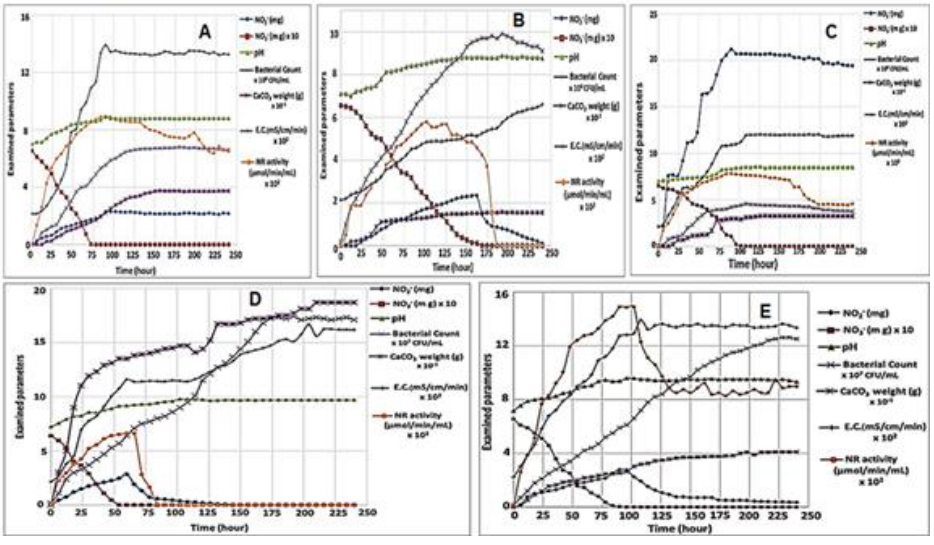

725

726

727

728

729

730

731

732

733

734

735

736

737

https://doi.org/10.5194/bg-2019-444
Preprint. Discussion started: 16 December 2019
© Author(s) 2019. CC BY 4.0 License.

738

739

740

741

742

743

744

745

746

747

748

749

750

751

752

753

754

755

Figure 4

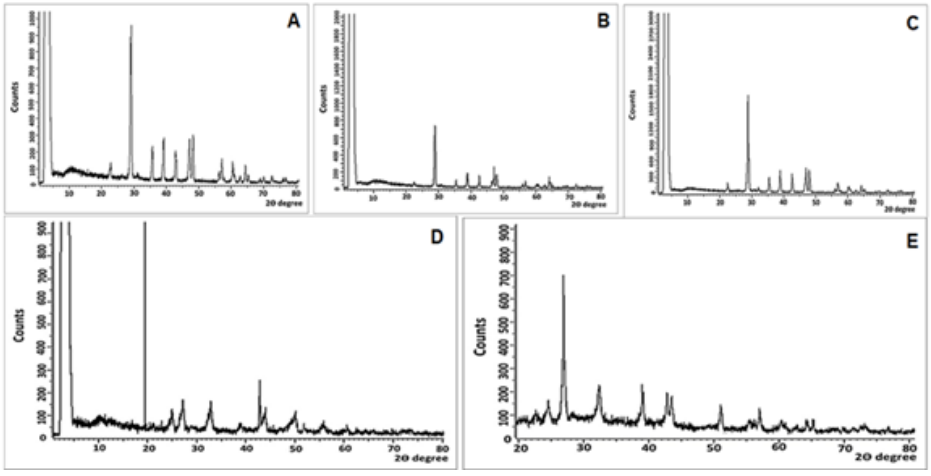

https://doi.org/10.5194/bg-2019-444
Preprint. Discussion started: 16 December 2019
© Author(s) 2019. CC BY 4.0 License.

Figure 5

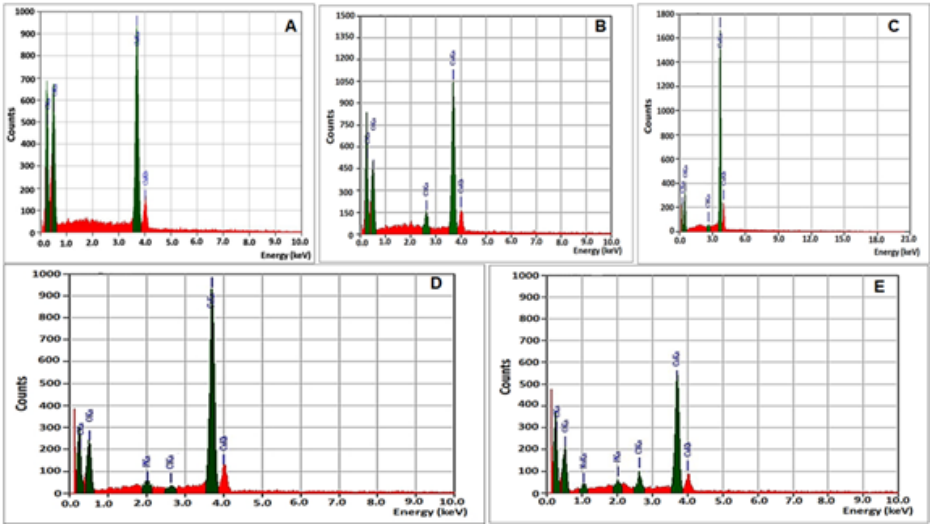

https://doi.org/10.5194/bg-2019-444
Preprint. Discussion started: 16 December 2019
© Author(s) 2019. CC BY 4.0 License.

774

775

Figure 6

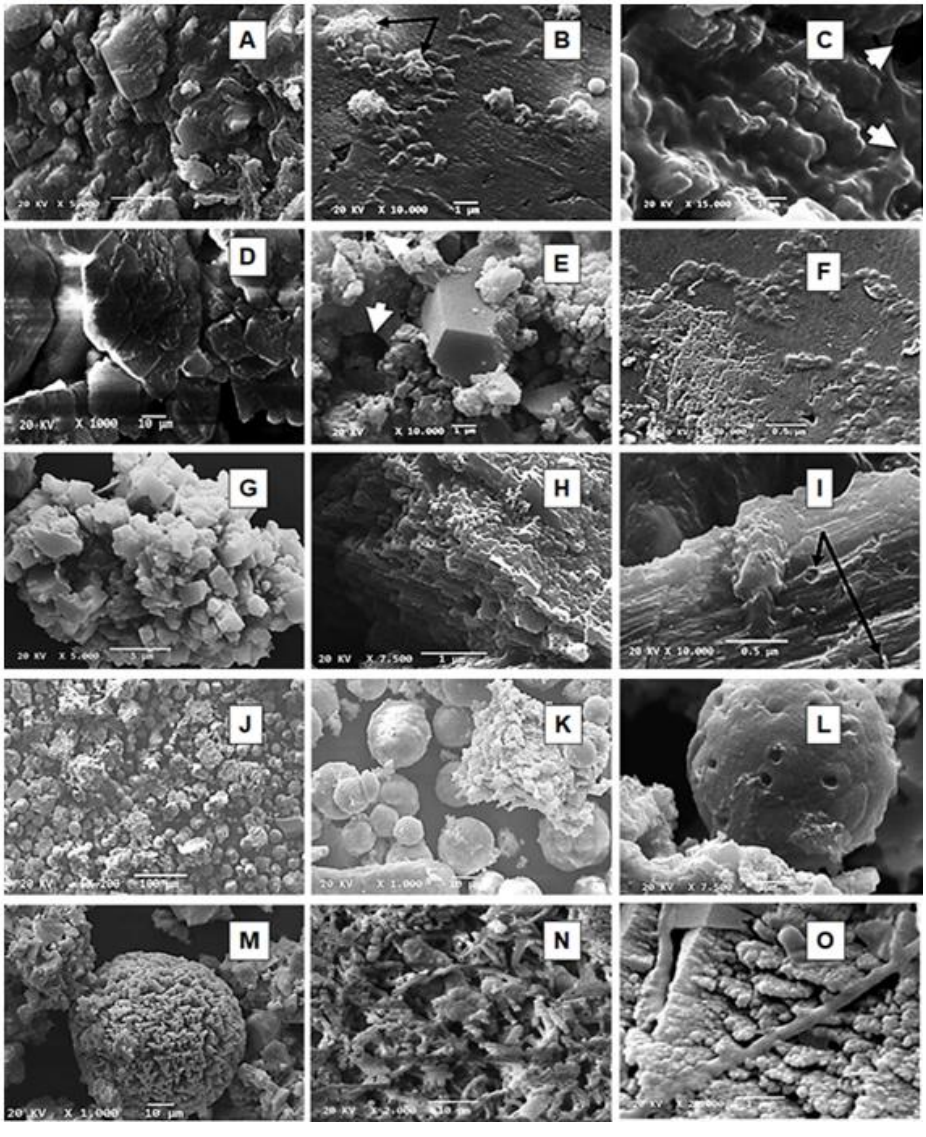

776

777

778

779

780

781

782

783

784

785

786

787

788

789